Available online at www.sciencedirect.com
ScienceDirect
Physics Letters B 640 (2006) 18–22
PHYSICS LETTERS B
www.elsevier.com/locate/physletb

First evidence of fusion hindrance for a small Q-value system

C.L. Jiang [a,*], B.B. Back [a], H. Esbensen [a], R.V.F. Janssens [a], Ş. Mişicu [a], K.E. Rehm [a], P. Collon [b], C.N. Davids [a], J. Greene [a], D.J. Henderson [a], L. Jisonna [a,c], S. Kurtz [b], C.J. Lister [a], M. Notani [a,d], M. Paul [e], R. Pardo [a], D. Peterson [a], D. Seweryniak [a], B. Shumard [a], X.D. Tang [a], I. Tanihata [a,1], X. Wang [a], S. Zhu [a]

[a] *Argonne National Laboratory, Argonne, IL 60439, USA*
[b] *University of Notre Dame, Notre Dame, IN 46556, USA*
[c] *Northwestern University, Evanston, IL 60208, USA*
[d] *Michigan State University, East Lansing, MI 48824, USA*
[e] *Hebrew University, Jerusalem 91904, Israel*

Received 1 June 2006; accepted 3 July 2006

Available online 14 July 2006

Editor: V. Metag

Abstract

The excitation function for the fusion–evaporation reaction $^{28}\mathrm{Si} + {}^{64}\mathrm{Ni}$ has been measured down to a cross section of 25 nb. This is the first observation of fusion hindrance at extreme sub-barrier energies for a system with a small, negative Q-value (-1.78 MeV). This result is further proof that heavy-ion fusion hindrance, reported earlier only for systems with large, negative Q-values, is a general phenomenon. The measured behavior can be reproduced by coupled-channels calculations with a modified ion–ion potential incorporating the effects of nuclear incompressibility.

PACS: 25.70.Jj; 24.10.Eq; 26.30.+k

The phenomenon of sub-barrier fusion enhancement in heavy-ion induced reactions at energies in the vicinity of the Coulomb barrier has been well documented for many systems [1–7]. In contrast, the unexpected hindrance of heavy-ion fusion at extreme sub-barrier energies has only been discovered more recently [8–12]. Indeed, it has been shown that the excitation functions of such reactions exhibit an abrupt decrease in cross section at the lowest beam energies and, as a result, a maximum appears in the associated astrophysical S factor at energy E_s [9]. This behavior cannot be described by conventional coupled-channels calculations. A new mechanism was proposed in Ref. [13], which explains heavy-ion fusion hindrance quite well for the fusion reaction $^{64}\mathrm{Ni} + {}^{64}\mathrm{Ni}$. In this model, the steep falloff of fusion is related to the saturation properties of nuclear matter which inhibit the large overlap of the reaction partners, cause a change of the nuclear potential inside the barrier and result in a hindrance of the quantum tunneling.

Thus far, the study of the sub-barrier hindrance phenomenon has focused solely on colliding systems with very negative fusion Q-values. As a result, the S factor must always reach a maximum at sufficiently low beam energies (corresponding to an abrupt decrease in the measured cross sections) since the final state phase space disappears when the center-of-mass energy, E, approaches $-Q$ [9]. The systematic study of Ref. [14] suggested, on the basis of a phenomenological analysis, that the hindrance behavior might be a general phenomenon in extreme sub-barrier fusion reactions, but this has not yet been demonstrated convincingly for a system with either a small negative Q-value, or even a positive one.

* Corresponding author.
E-mail address: jiang@phy.anl.gov (C.L. Jiang).
[1] Present address: TRIUMF, 4004 Wesbrook Mall, Vancouver, BC, V6T2A3, Canada.

0370-2693/$ – see front matter © 2006 Published by Elsevier B.V.
doi:10.1016/j.physletb.2006.07.007

In order to explore this issue, the fusion–evaporation excitation function for the $^{28}Si + {}^{64}Ni$ system with a Q-value of only -1.78 MeV has been measured down to 25 nb. This represents a qualitative difference from the well studied systems mentioned above, where the Q-values ranged from -36.6 MeV for $^{32}S + {}^{89}Y$ [15] to -157.4 MeV for $^{90}Zr + {}^{90}Zr$ [16]. Furthermore, the present study also represents an opportunity to investigate whether the ion–ion potential used in Ref. [13] is able to describe fusion systems much lighter than the one discussed in the earlier work. It should be noted that this $^{28}Si + {}^{64}Ni$ system had been measured previously down to a cross section of 41 μb [17], i.e., down to an energy insufficient to investigate the issue under discussion here.

The experiment was performed with ^{28}Si beams in the energy range of 63–95 MeV delivered by ATLAS, the superconducting linear accelerator at Argonne National Laboratory. The maximum beam current used was ∼100 pnA. This relatively high beam intensity does not represent a problem in terms of target damage because of the high melting point of the highly-enriched, metallic nickel material (which was evaporated on a 40 μg/cm^2 carbon foil). Thin targets with thicknesses of about 15 μg/cm^2 were used in order to reduce the correction for target thickness in the energy regime where the steep fall-off in the excitation function occurs. The isotopic abundance of ^{64}Ni was 98.02%, with the remainder coming from ^{58}Ni (0.97%), ^{60}Ni (0.57%), ^{61}Ni (0.05%) and ^{62}Ni (0.39%). Small contaminations from lighter isotopes did not interfere with the actual measurements since the associated barriers are all higher than for ^{64}Ni. Two surface-barrier Si detectors, located at ±43° with respect to the beam direction, served as monitors. The absolute cross sections for fusion–evaporation were determined by using elastic scattering measured with these two counters.

The experimental procedure was similar to that used in earlier measurements of the fusion–evaporation excitation function for the system $^{64}Ni + {}^{100}Mo$ [11,18]. Briefly, the evaporation residues were measured with the Fragment Mass Analyzer (FMA) [19] placed at 0° with respect to the beam direction. The instrument has been upgraded with the installation of a split-anode in the first electric-dipole [20]. The background, originating mostly from the beam scattered off the first anode, is greatly suppressed as a result. The evaporation residues were detected and identified behind the FMA with detectors of the configuration $PGAC_1$–TIC_1–$PGAC_2$–TIC_2–$PGAC_3$–IC described in detail in Ref. [18]. Here, the symbol PGAC stands for an x–y position sensitive, parallel-grid avalanche counter, TIC for a transmission ionization chamber, and IC for a large volume multi-anode ionization chamber. The first $PGAC_1$ was mounted at the horizontal (x-direction) focal-plane of the FMA, where the evaporation residues are dispersed according to their mass-to-charge ratio m/q.

Only one charge state at the time could be measured at each FMA setting. As a result, full charge state distributions were obtained at five energies, while three to five charge states were recorded for five intermediate points. Only one charge state was measured for the six lowest energies because of the low cross sections involved. These data proved sufficient to determine the charge state fractions of the detected evaporation residues with the desired accuracy.

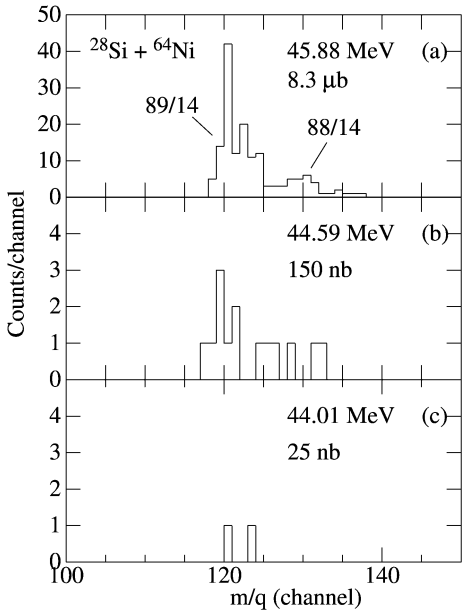

Fig. 1. m/q spectra obtained at three of the lowest bombarding energies for $^{28}Si + {}^{64}Ni$ fusion evaporation residues. The corresponding fusion evaporation cross sections were 25 nb, 150 nb and 8.3 μb, respectively. The peaks observed in (a) are for $m/q = 89/14$ (low channel number) and 88/14, respectively.

In order to establish the FMA transmission, it is necessary to characterize the angular distribution of the residues. In the present experiment this was achieved by determining their velocity distribution. This method was developed at Argonne previously [21] and relies on an accurate determination of the time of flight of the reaction products on an event-by-event basis. For this purpose the flight time from the target to $PGAC_1$, and the flight time between $PGAC_1$ and $PGAC_3$ were used. The inferred angular distributions agreed well within the desired uncertainty with that measured at $E_{lab} = 84.5$ MeV in Ref. [17], as well as with those calculated with the statistical code PACE [22].

The separation between the evaporation residues and the background was very good even at the lowest energy measured. Three position-spectra are given for the measurements carried out at the lowest, 2nd-lowest and 4th-lowest energies in Fig. 1. The peaks observed in Fig. 1(a) correspond to residues with $m/q = 89/14$ (lower channel number) and 88/14, respectively. At the lowest-energy, two evaporation residues with $m/q = 89/14$ were observed. The fusion evaporation cross sections measured at these three energies were 25 nb, 150 nb and 8.3 μb, respectively.

The experimental cross sections, covering more than 7 orders of magnitude, are presented in Fig. 2, as an excitation function in the center-of-mass system. Comparisons with the previous data [17] are provided as well. In the near-barrier region, the two measurements agree within experimental uncertainties. At lower energies, however, an energy shift $\Delta E_{lab} \sim 1.2$ MeV between the two data sets appears; the situation is similar to that found earlier for fusion in the $^{64}Ni + {}^{64}Ni$ system. In this case as

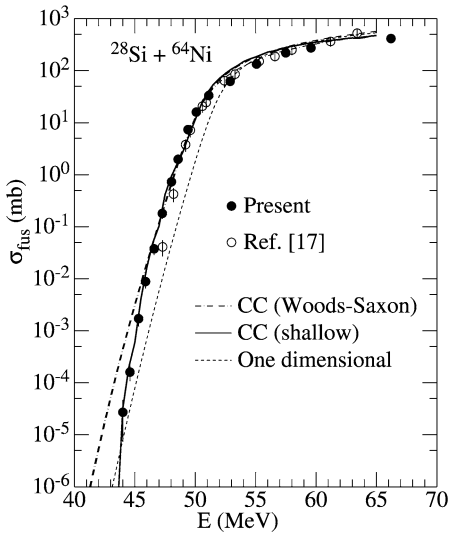

Fig. 2. Excitation function for the fusion of ^{28}Si + ^{64}Ni. The solid circles are the present results, while the open ones are taken from Ref. [17]. The dot-dashed and solid curves are the results of coupled-channels calculations with a usual Woods–Saxon potential and a shallow potential incorporating the effects of nuclear incompressibility, respectively (see text for details). The dotted curve is the result of a one-dimensional, no-coupling calculation.

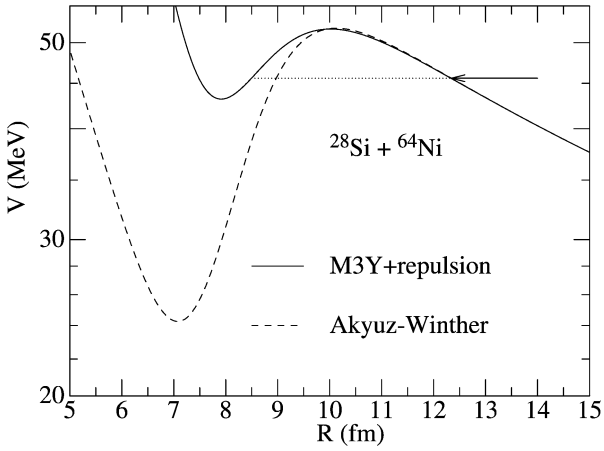

Fig. 3. Spherical ion–ion potentials for ^{28}Si + ^{64}Ni; the solid curve is the potential employed in the present study. The dashed curve is the Akyüz–Winther potential. The horizontal solid and dotted lines are schematical plots of the trajectories for incident ions at an energy $E = E_s$.

well, an energy shift $\Delta E_{\rm lab} \sim 1.5$ MeV was observed between the cross sections measured at Argonne [10] and those reported in Ref. [23].

Detailed coupled-channels calculations have been carried out in order to account for the data. As a starting point, they took advantage of the fact that the earlier data of Ref. [17] had been analyzed in the coupled-channels approach [24]. Specifically, sensitivity to transfer reactions was found, in particular to 2-neutron transfer, a process with a positive ground-state Q-value of 2.59 MeV. The present calculations are similar to those of Ref. [24] for the coupled-channels part. Thus, they include the 2^+ and 3^- excitations in both ^{28}Si and ^{64}Ni, the mutual excitations below 7 MeV and the two-phonon quadrupole excitations. All together, ten channels were coupled. Two types of potentials were considered. The first was a conventional Woods–Saxon ion–ion potential with a diffuseness parameter $a = 0.63$ fm. In order to reproduce the present data in the cross section range above 0.2 mb, the radius parameter $\Delta R = 0.20$ fm used in Ref. [17] had to be adjusted to 0.31 fm. The coupled-channels calculations, together with a one-dimensional penetration calculation (without couplings) can be seen in Fig. 2 as dot-dashed and dotted curves, respectively. As in previous studies [8–12], the conventional coupled-channels calculations (with a Woods–Saxon potential) reproduce the data well for all cross sections above ∼0.1 mb, but overpredict the measurements at extreme sub-barrier energies.

As stated above, a new mechanism was proposed to explain fusion hindrance at extreme sub-barrier energies by considering explicitly the incompressibility of the overlapping reaction partners and estimating the ion–ion potential in a double folding model [13]. The inclusion of this compressional energy results in a shallower potential and thicker barriers, that is ultimately responsible for the fast fall-off of the excitation function at the lowest beam energies. The same approach was adopted to analyze the present experiment. The potential proposed in Ref. [13] (M3Y + repulsion) is compared with a more conventional Woods–Saxon one (Akyüz–Winther [25]) in Fig. 3, where the schematic trajectories of particles of energy $E = E_s$ is also indicated.

The coupled-channels calculation results with this shallow potential are given by the solid curve in Fig. 2. The agreement between the model and the data is satisfactory and of the same order as in the ^{64}Ni + ^{64}Ni case. Thus, a consistent interpretation is achieved for two systems with strikingly different Q-values, as the rather small negative Q-value, −1.78 MeV, for the fusion reaction ^{28}Si + ^{64}Ni does not appear to affect the ability to reproduce fusion hindrance at extreme sub-barrier energies.

The logarithmic derivatives $L(E)$ and the S factor have also been derived using the expressions given in Ref. [9]. These two quantities are shown in Figs. 4(a) and 4(b), respectively. In Fig. 4(a) the star symbols are obtained from a least squares fit to three neighboring entries for the cross sections. The heavy solid line in the figure is the so-called constant S factor expression, $L_{cs}(E) = \frac{\pi\eta}{E}$, derived in Ref. [9], while the dotted line corresponds to a linear fit to the low-energy part of $L(E)$. The crossing point of these two lines determines the location of the maximum in the S factor curve, which occurs at $E_s = 45.6$ MeV and $L_s = 2.78$ MeV^{-1} for the ^{28}Si + ^{64}Ni system. It is worth noting that, from the previous data (Ref. [17]), a value of $E_s = 47.3$ MeV is obtained with the extrapolation method described in [9]. The difference in the values extracted from the two measurements is due to the combination of the energy shift in the excitation functions mentioned above and the precise knowledge of the fall-off of the cross section that is now available. The data for $L(E)$ and $S(E)$ deduced from Ref. [17] are given as open circles in Figs. 4(a) and 4(b) for comparison.

Obviously, there is a significant, but broad maximum in the S factor curve as a function of energy (see Fig. 4(b)). This behavior cannot be reproduced by the calculations based on the Woods–Saxon potential (dot-dashed curves). On the other hand,

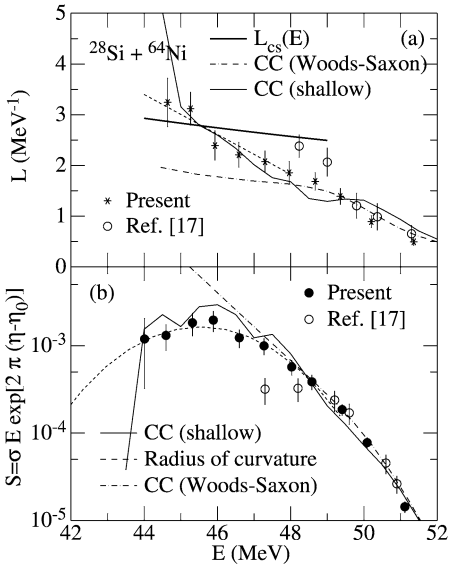

Fig. 4. (a) The logarithmic derivative $L(E) = d(\ln \sigma E)/dE$, plotted as a function of the center-of-mass energy E for the fusion of $^{28}\mathrm{Si} + {}^{64}\mathrm{Ni}$. The stars are obtained from least squares fits to three data points. (b) The S factor $S(E) = \sigma E \exp(2\pi\eta)$, plotted as a function of the center-of-mass energy E. The solid circles are the experimental results. The $L(E)$ and $S(E)$ values obtained from the data of Ref. [17] are shown as open circles. The heavy solid line corresponds to a constant S factor. See text for details.

the new potential by using the recipe of Ref. [13] (solid curves) follows the patterns exhibited by the data.

The extracted values for the parameters L_s and E_s in the reaction $^{28}\mathrm{Si} + {}^{64}\mathrm{Ni}$ are described well by the empirical expressions given in Ref. [14]:

$$L_s^{\mathrm{emp}} = 2.33 + 500/\left(Z_1 Z_2 \sqrt{\mu}\right) \left(\mathrm{MeV}^{-1}\right), \tag{1}$$

and

$$E_s^{\mathrm{emp}} = \left(0.495 Z_1 Z_2 \sqrt{\mu}/L_s^{\mathrm{emp}}\right)^{2/3} (\mathrm{MeV}), \tag{2}$$

within the desired accuracy. The derivatives $(dL/dE)_{\mathrm{exp}}$ and $(dL/dE)_{cs}$ obtained at E_s are -0.39 and -0.09 MeV^{-2}, respectively. The general trend exhibited by the ratio of these two derivatives is also described well by another empirical equation proposed in Ref. [14],

$$\mathrm{Ratio}^{\mathrm{emp}} = 1 + 10^{-5}\left(Z_1 Z_2 \sqrt{\mu}\right)^{5/3}, \tag{3}$$

where μ is the reduced mass number $A_1 A_2/(A_1 + A_2)$.

All these observations confirm the conclusion proposed in Ref. [12], that the systematic behavior of the hindrance phenomenon is closely related to the properties of the entrance channel of the colliding system.

As mentioned above the maximum of the S factor of the fusion reaction $^{28}\mathrm{Si} + {}^{64}\mathrm{Ni}$ is broad. Since

$$\frac{d^2 \ln(S(E))}{dE^2} = \frac{dL(E)}{dE} - \frac{d(\frac{\pi\eta}{E})}{dE}, \tag{4}$$

the radius of curvature ρ of $\ln(S(E))$ vs. E can be expressed as,

$$\frac{1}{\rho} = \frac{dL(E)}{dE} - \frac{d(L_{cs}(E))}{dE}. \tag{5}$$

Thus, ρ is determined by the difference between the derivative of $L(E)$ and that associated with a constant S factor $(dL/dE)_{cs}$ at $E = E_s$. Expanding to second order around the S factor maximum we thus find

$$S(E) = S(E_s) \times e^{(E-E_s)^2/2\rho}, \tag{6}$$

as shown by the dashed curve in Fig. 4(b). It describes the experimental $S(E)$ values at energies $E \sim E_s$ rather well. It should be mentioned that in comparison with the medium-mass fusion systems where Q-values are large and negative, the absolute value of $\frac{dL(E)}{dE} - \frac{d(L_{cs}(E))}{dE}$ for the $^{28}\mathrm{Si} + {}^{64}\mathrm{Ni}$ reaction is smaller, and the absolute value of ρ is larger, resulting in a $S(E)$ factor with a broader maximum. This observation also holds for other systems with small negative Q-value, although their $S(E)$ maxima have not yet been explored as thoroughly as is the case for the reaction under study here. Nevertheless this behavior can already be seen by using the extrapolation method developed in Ref. [10].

This work has reported on the first observation of sub-barrier fusion hindrance, and a clear maximum in the S factor as a function of energy, in a colliding system with a near zero Q-value. This result confirms the assumption made previously that the sub-barrier hindrance is a general phenomenon in heavy-ion reactions. Furthermore, the success of the comparison of the new data with the model proposed in Ref. [13] can be viewed as further evidence that the hindrance is a consequence of the modification of the ion–ion potential inside the barrier originating from the incompressibility for total overlap between the reaction partners. Because this phenomenon manifests itself at the lowest energies, it is expected to impact stellar processes significantly and should be incorporated in network calculations involving fusion of light heavy-ion reactions which are of interest in astrophysics [26].

Acknowledgements

This work was supported by the US Department of Energy, Office of Nuclear Physics, under contract No. W-31-109-ENG-38. One of the authors (Ş. Mişicu) is grateful to the Fulbright Commission for financial support.

References

[1] M. Beckerman, Phys. Rep. 129 (1985) 145.
[2] M. Beckerman, Rep. Prog. Phys. 51 (1988) 1047.
[3] K. Hagino, N. Takigawa, M. Dasgupta, D.J. Hinde, J.R. Leigh, Phys. Rev. C 55 (1997) 276.
[4] A.B. Balantekin, N. Takigawa, Rev. Mod. Phys. 70 (1998) 77.
[5] R. Vandenbosch, Annu. Rev. Nucl. Part. Sci. 42 (1992) 447.
[6] N. Rowley, G.R. Satchler, P.H. Stelson, Phys. Lett. B 254 (1991) 25.
[7] M. Dasgupta, D.J. Hinde, N. Rowley, A.M. Stefanini, Annu. Rev. Nucl. Part. Sci. 48 (1998) 401.
[8] C.L. Jiang, et al., Phys. Rev. Lett. 89 (2002) 052701.
[9] C.L. Jiang, H. Esbensen, B. Back, R.V.J. Janssens, K.E. Rehm, Phys. Rev. C 69 (2004) 014604.
[10] C.L. Jiang, et al., Phys. Rev. Lett. 93 (2004) 012701.
[11] C.L. Jiang, et al., Phys. Rev. C 71 (2005) 044613.
[12] For system $^{58}\mathrm{Ni} + {}^{89}\mathrm{Y}$, C.L. Jiang, et al., ANL Phys. Div. Annual Report ANL-05/61, p. 81.

[13] Ş. Mişicu, H. Esbensen, Phys. Rev. Lett. 96 (2006) 112701.
[14] C.L. Jiang, B. Back, H. Esbensen, R.V.J. Janssens, K.E. Rehm, Phys. Rev. C 73 (2006) 014613.
[15] A. Mukherjee, et al., Phys. Rev. C 66 (2002) 034607.
[16] J.G. Keller, et al., Nucl. Phys. A 452 (1986) 173;
J.G. Keller, et al., Phys. Lett. B 254 (1991) 25.
[17] A.M. Stefanini, et al., Nucl. Phys. 456 (1986) 509;
A.M. Stefanini, et al., Phys. Rev. C 30 (1984) 2088.
[18] C.L. Jiang, et al., Nucl. Instrum. Methods A 554 (2005) 500.
[19] C.N. Davids, J.D. Larson, Nucl. Instrum. Methods B 40–41 (1989) 1224;
C.N. Davids, B.B. Back, K. Bindra, D.J. Henderson, W. Kutschera, T. Lauritsen, Y. Nagame, P. Sugathan, A.V. Ramayya, W.B. Walters, Nucl. Instrum. Methods B 70 (1992) 358.
[20] C.N. Davids, ANL Phys. Div. Annual Report ANL-03/23, 2003, p. 104.
[21] C.L. Jiang, et al., ANL Phys. Div. Annual Report ANL-97/14, p. 55.
[22] A. Gavron, Phys. Rev. C 21 (1980) 230.
[23] D. Ackermann, et al., Nucl. Phys. A 609 (1996) 91.
[24] S. Landowne, S.C. Pieper, F. Videbaek, Phys. Rev. C 35 (1987) 597.
[25] R.A. Broglia, A. Winther, Heavy Ion Reactions, Lecture Notes the Elementary Process, vol. 1, Addison–Wesley, CA, 1991, p. 114.
[26] C.L. Jiang, K.E. Rehm, B. Back, H. Esbensen, R.V.J. Janssens, in preparation.